Astron. Astrophys. 259, L61–L64 (1992)

ASTRONOMY
AND
ASTROPHYSICS

Letter to the Editor

3C 179: a high fidelity image of the double-lobed superluminal quasar at 5 GHz

C. E. Akujor[1,2]

[1] Onsala Space Observatory, S-439 00, Sweden
[2] Nuffield Radio Astronomy Laboratories, Jodrell Bank, Cheshire SK11 9DL, England

Received March 10, accepted March 24, 1992

Abstract. We present a high fidelity image of the powerful double-lobed superluminal quasar 3C179 made with MERLIN at 5 GHz. It has a knotty one-sided jet which appears to be disrupted at a 'splash' knot. Its asymmetric structure can be explained within the relativistic beaming hypothesis if the jet has slowed after the disruption. We infer that the jet is inclined at $\sim 12° - 23°$ to the line sight with a speed $\sim 0.6 - 0.8c$. This is compatible with hotspot advance speed $\sim 0.02c$, so we need not invoke relativistic considerations to explain the hotspot asymmetry.

Key words: Quasars: 3C179 - quasars: jet

1. Introduction

3C179 (alias 0723+679) is a powerful quasar with a double-lobed radio structure (with redshift z=0.846; Wills & Wills 1976) and is the first double-lobed extra-galactic object and one of the first few radio sources in which superluminal motion was detected (with apparent speed, $v_{app} = 4.8c$; Porcas 1981, 1986). It has a prominent kpc-jet and a core component, which although bright relative to other double-lobed quasars of the same intrinsic luminosity still accounts for less than 50% of the total flux density at 5 GHz (see Pearson, Readhead & Barthel 1987).

3C179 has been the subject of intense investigation, but previous efforts have largely been concentrated on the mas jet (Porcas 1987) and the overall large-scale structure (Owen & Puschell (1984). The detailed structure of the kpc-scale jet of 3C179 and many other extended jet sources have rarely been investigated in detail because the majority of them are too large for simple MERLIN observations at 5 GHz and can only be investigated with the VLA at very high frequencies where these jets could be very faint.

In this letter, we present a high fidelity image of 3C179 obtained with MERLIN at 5 GHz. The high resolution and extraordinary fidelity achieved on this image enables us to reveal fine details of the structure of both the jet and other bright features of the radio structure. The relationship between the asymmetric structure and orientation of the source is discussed within the relativistic beaming theory. (We work in the domain of Einstein- de-Sitter universe with $H_o = 100 kms^{-1} Mpc^{-1}$, $q_o = 0.5$; so that $1 arcsec = 4.2 kpc$).

*on leave from University of Nigeria, Nsukka, Nigeria

2. Observations and Data reduction

The observations were made on 15 – 17 April 1982 with the MERLIN array (Thomasson, 1986). These were extended track observations of about 42 hours with five of the antennae of the MERLIN array (MK2, Darnhall, Defford, Tabley and Knockin). The radio source DA193 (0552+398), which is unresolved on all baselines, was used for correcting the correlator-based closure offsets and the flux density was established with observations of 3C286 on the scale of Baars *et al.* (1977).

The data calibration and initial processing were made in the Jodrell Bank OLAF package. The mapping was essentially done using the OLAF difference-mapping routine, "MAP" which employs the self-calibration technique (Cornwell & Wilkinson 1981). After a few initial mapping iterations, the processed data were then transfered to AIPS where we then phase-calibrated using VLA data (J. Conway, private comm.), then the MX routine was used to obtain clean components which were then taken back to OLAF as a model for final mapping. The data were 'tapered' to increase the sensitivity and stress some of the low brightness features, as well as to put the entire structures in one map, since OLAF does not accommodate multiple field mapping. The advantages of having *apriori* knowledge of the overall radio structure from VLA observations (J. Conway, private comm; Owen & Puschell 1984), the long track observation, the careful editing to remove obvious bad uv data points and the use of clean components obtained in AIPS as a model and multiple clean windows (up to 30 at a time) in OLAF 'MAP' resulted in a high quality image – one of the best images made with MERLIN at 5 GHz.

3. Results

The final image of 3C179 made with a 150 mas circular beam is shown in Fig 1 (inset is a 408 MHz map which is a reanalysis of Shone *et al.* (1985) data). The lowest contour in the map is 0.3 mJy/beam. This map is broadly consistent with earlier MERLIN and VLA maps at 1.6 GHz (Shone *et al.* 1985) and 5 GHz (Owen & Puschell, 1984) respectively. The different components of this source have been clearly resolved in our map. This map shows a bright core and a kpc-scale jet. The eastern lobe appears to have a filamentary structure which could be due to poor uv coverage of the MERLIN observations, but such filamentary structure has been seen in the lobes of Cygnus A and other powerful radio sources (e.g. Perley *et al.* 1984; Akujor & Garrington 1991).

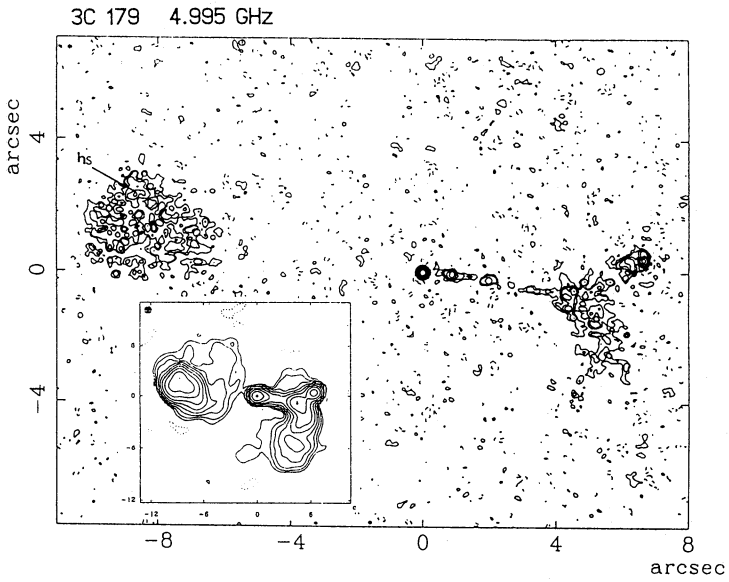

Fig. 1. Merlin map of 3C179 at 5 GHz. The contour levels are at -0.2, -0.1, 0.1, 0.2, 0.4, 0.8, ...% of the peak brightness, 308 mJy/beam; the restoring beam is 150 mas (circular). Inset is a 408 MHz map; restoring beam is 1 arcsec.

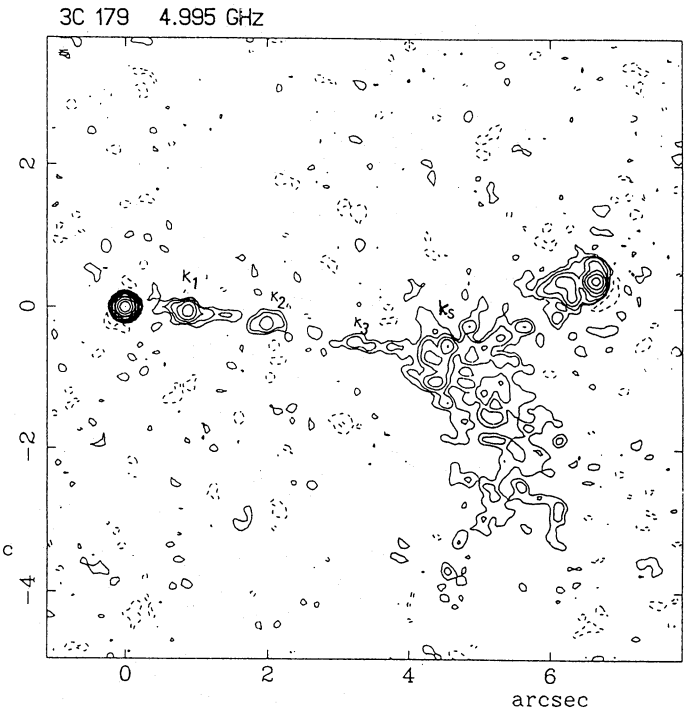

Fig. 2. A close–up of the core-jet side of 3C179 at 5 GHz

The northern tip of this lobe contains a weak hotspot. The flux densities of the eastern and western hotspots are 25.6 and 55.6 mJy respectively, and they together account for 5 percent of the total flux density ($\sim$ 1300 mJy) of the source from single dish measurements (Kuhr *et al.* 1981). The total flux density in the jet is $\sim 70\,mJy$ which is $\sim$ 6% of the total flux density. There is no evidence of a counter–jet, but we put an upper limit on the jet/counter–jet ratio, D of $\geq 25:1$, which is the ratio of peak brightness in the jet (as measured in the brightest knot, K_1 which is before the splash at K_S) to $3\sigma_{rms}$. The core has a flux density of 309 mJy, which is $\sim$ 24% of the total flux density. The core–to–extended flux density ratio, R is therefore 0.3.

Fig 2 is a close–up on the core and the jet–side. The jet has three main knots before the 'splash' knot K_S where it is apparently disrupted, splitting into two parts. It is well–collimated within this initial 18.7 kpc before knot K_S and beyond this point the brighter deflected 'branch' appears to be decollimated or to expand leading up to a bright terminal hotspot. The weaker 'branch' of the jet to the Southwest appears to fade gently into the extended lobe structure seen at low frequencies (see inset to fig 1). The flux densities of knots K_1, K_2, and K_3 are $\sim$ 16, 6, 3 mJy respectively, while the total flux density in splash knot K_S is 35 mJy.

4. Discussion

Do knot K_S and the terminal hotspot constitute a normal hotspot complex comprising a 'primary' and 'secondary' hotspot as is common in other powerful quasars (Lonsdale & Barthel 1984, 1986)? The consensus concerning the formation of double hotspots seems to be converging (Lonsdale & Barthel 1986, Laing 1989, Lonsdale 1989) on a model in which the bright and more compact primary hotspot is formed by the impact of the extended jet on the side wall of a cavity. A collimated outflow of plasma from the primary is then directed to form the secondary hotspot from which 'processed' material then flows into extended lobes and cocoons. It then follows that the general trend is for the jet to be more closely aligned with and connected to the primary hotspot than the secondary. This model does not apply in 3C179 regarding the relationship between knot K_S and the terminal hotspot. The well–collimated jet leads directly into a weaker knot K_S and goes on to form a bright hotspot at the end. The edge–brightening of the hotspot which is absent in knot K_S is an indication that it is indeed a 'working surface' in the interaction of the jet with ambient cavity. Knot K_S does not qualify as a secondary hotspot as it is in the path of the jet before the terminal hotspot and does not appear to be formed by material already processed in the bright hotspot. Moreover, most of the lobe material appears to originate principally from knot K_S well before the formation of the terminal hotspot.

We believe the jet in 3C179 is disrupted and split at knot K_S for the following reasons. It is well collimated before knot K_S ($\sim 18kpc$ from the nucleus), but beyond that it has two distinct directions of outflow, the brighter 'branch' of the jet which also shows evidence of expansion or decollimation leading up to the terminal hotspot and the weaker and more diffuse branch towards the SW. Also, the magnetic field directions infered from VLA polarisation images (Owen & Puschel, 1984; I. Browne, private comm.) indicate material flow in the directions of the two 'branches' of the jet beyond knot K_S. There is, also, a rather circumstantial evidence in the absence of a secondary hotspot 'arising' from the 'primary' terminal hotspot. This could indicate that after the 'splash' at knot K_S the jet power is so degraded that it is unable to 'bounce' off to form a secondary hotspot.

The disruption of the jet on a scale longer than the typical galactic size (*i.e* possibly outside the confines of the host galaxy ISM) can be explained by interaction with dense gaseous matter

in the IGM. Such dense gas will be filamentary to split the jet into two parts. The expansion of the jet will then arise from pressure gradient in the IGM (see Chan & Henricksen 1980) or the transfer of jet momentum to the ambient medium due to viscous interaction (see Baan 1980, Hardee 1982). The jet will also slow down to due to momentum loss. The existence of this dense gas has been confirmed by McCarthy (1989) who find that line–emitting gas is always associated with the shorter side of powerful sources. This explains why the jet side is unexpectedly shorter than the counter–jet side. Moreover, that filaments and clouds of emission–line gas exist in powerful sources on the scale of $10 - 100kpc$ has been confirmed by van Breugel *et al.* (1985).

Indeed the structure of the jet in 3C179 has some close resemblance to that seen recently in 3C48 (Wilkinson *et al.* 1991) a quasar whose radio structure is buried deep within the host galaxy. If the jet disruption in 3C48 is indeed due to collision with a dense gas clump in the ISM of the host galaxy as suggested by Wilkinson and colleagues, observation of similar features in the 3C179 jet at $\sim 18kpc$ from the core, possibly outside the confines of the host galaxy has implications for the kpc–scale jet structure in powerful radio sources. It may be telling us that the structure seen in radio sources on all scales is determined to a large extent by the nature of the ambient medium and that clumpy gas exists in both the ISM of host galaxies and the surrounding IGM.

In the context of the relativistic twin–beam model (Scheuer & Readhead 1979), the ratio of the intensities in the approaching and receding components (jet/counter–jet ratio), D is expected to be;

$$D = ((1 + \beta\cos\theta)/(1 - \beta\cos\theta))^{2+\alpha}$$

where we assume that the angle with respect to the line of sight, θ and the spectral index α ($S \propto \nu^{-\alpha}$) are the same for the jet and the counter–jet. The corresponding Lorentz factor, γ, is given by

$$\gamma = ((1 - 1/\cos^2\theta)((D^x - 1)/(D^x + 1))^2)^{-0.5}$$

where $x = 1/(2 + \alpha)$. We assume $\alpha = 0.6$ in the jet, and obtain $\beta\cos\theta \geq 0.67$ for the lowest value of D=25. But the exact value of D is unknown and in principle can be very large. The variation of θ with γ for a range of D (25, 100, 400, 1600, 6400) has been calculated and shown in Fig.3. But we have information on motion in the core where superluminal motion, $\beta_{app} = 4.8$ has been measured (Porcas 1981, 1986,a, 1987). The apparent speed in the core, β_{app} is related to the inclination angle θ thus;

$$\beta_{app} = \beta sin\theta/(1 - \beta\cos\theta)$$

which in this case translates to;

$$\gamma = 1/(1 - (4.8/(\sin\theta + 4.8\cos\theta))^2)^{0.5}$$

The possible values of θ with corresponding γ values are also plotted in Fig. 3. We note that the actual value of the superluminal speed depends on the combinations of the values of the decceleration parameter, q_o and the Hubble constant, h in units of $100kms^{-1}Mpc^{-1}$. We use a rather conservative combination of $h = 1$ and $q = 0.5$.

We can put another constraint on the range of θ from the Orr & Browne (1982) scheme which attributes the observed differences between flat– and steep–spectrum quasars to the effects of projection and the relativistic amplification of the nuclear components. It provides a relationship between the ratio, R, of the luminosity of the core to that of the extended structure, $R_T = R(90^0)$, and θ thus:

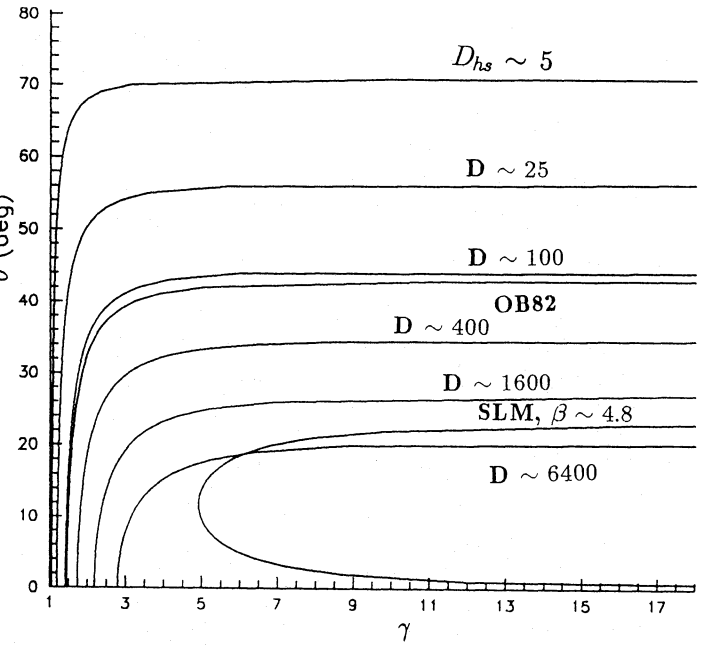

Fig. 3. Plot of variation of θ with γ for the jet in 3C179 for the various model

$$R = 1/2R_T((1 - \beta\cos\theta)^{-2} + (1 + \beta\cos\theta)^{-2})$$

For 3C179 we measure R=0.3 and for $R_T = 0.024(1 + z)$ (see Orr & Browne 1982), we obtain a range of values of β and hence γ for different possible values of θ. This is also shown as a curve (OB2) in Fig 3. Although the Orr & Browne scheme refers to the mas jet since the core boosting arises mainly from there, the obtained $\beta - \gamma$ distribution corresponds exactly to the same we would obtain in the relativistic beaming model for the kpc jet for $D \sim 120$, with $\theta_{max} = 48°$. The fairly close alignment between the mas–scale and the kpc–scale jets (see Porcas, 1984, 1986) is an indication that θ should not differ significantly for the jet on different scales.

Why do we obtain a $\theta - \gamma$ distribution for the mas jet from the Orr & Browne scheme that is different from that derived from consideration of the observed superluminal motion? We suggest some possibilities that a) superluminal motion is observed in the first few mas ($\sim 10mas$ in this case) from the core, while the Orr & Browne scheme refers to the entire core which in this case is of the scale of a half of the beam size $\sim 150/2mas$. The jet could have slowed down far from the mas core region resulting in an overall low γ value, b) the measured core luminosity could be contaminated by isotropic diffuse emission with low γ which does not enter the flux budget at VLBI resolution, particularly at high frequency as in this case where the observations were made at 10 GHz, and c) it is possible, as has been suggested (e.g. Lind & Blandford 1985), that the superluminal motion we detect is related to a shock front in the jet, which could be different speed from that of the plasma. This does not necessarily change θ but requires that the γ be different from that derived from simple beaming calculations.

The range of θ for the jet will therefore be bound by γ_{min} and θ_{max} from superluminal motion, that is $\theta \sim 12° - 23°$. But we expect γ to be lower for the kpc jet than that of the nuclear jet, so the limit of the jet/counter–jet ratio in the kpc jet must be $D \sim 25 - 120$, the corresponding γ in the derived range of θ is therefore 1.2–1.6 ($\beta = 0.6 - 0.8$). So, although the mas–

scale jet in 3C179 is superluminal, the large–scale jet appears to be mildly relativistic. Moreover, the peak brightness of the counter–jet could be as low as $70\mu Jy/beam$ at 5 GHz.

The maximum brightness in the jet occurs in knot K_1 which is well before the apparent disruption, so speeds and angles we estimate refer to the jet before the disruption as this may well have degraded the jet speed and momentum. We however assume that the intrinsic orientation of the jet with respect to the observer does not change significantly. The ratio, d of the maximum separation of the two sides of the source is

$d = (1 + \beta_1 \cos\theta)/(1 - \beta_o \cos\theta)$

where β_o is for the counter-jet and $\beta_1 = b\beta_o$ is averaged over the jet side b, is the factor by which original jet speed is degraded by the disruption at knot K_5. For the extreme values of $\theta \sim 23$ and $\beta \sim 0.8$, we obtain $b \sim -0.4$. So to produce the observed asymmetry in lobe distance in 3C179 the average jet speed had to go down by more than half to $\sim 0.3c$ as a result of the splash at knot K_5. Note that this is averaged over the entire jet so that the terminal speed of the jet will be somewhat lower.

If relativistic conditions are considered, then the same relationship for jet brightness asymmetry may apply in the hotspot. In this case the ratio of the peak brightness of the 'approaching' and 'receding' hotspots, $D_{hs} = 5$, so that

$\beta_{hs} \cos\theta = (D_{hs}^x - 1)/(D_{hs}^x + 1)$

yields $\beta_{hs} \cos\theta = 0.29$. The variation of possible values of θ with corresponding values of γ is shown also in fig. 3. The minimum value of β is bound by $\theta = 0$, that is, $\beta_{hs} \geq 0.3$, since the hotspot need not have the same viewing angle as the jet. But the hotspot advance speed cannot be higher than the terminal jet speed, which is ≤ 0.3, so we think that the observed hotspot asymmetry could not *in this case* be due to the flow through the hotspot of relativistic amplified beam material, unless the hotspot is viewed directly end-on (at $\theta = 0$).

This is compatible with hotspot advance speed v_{hs} estimated classically from ram–pressure balance, given by (see Blandford & Rees 1974, Lonsdale & Barthel 1986);

$v_{hs} = (u_m/3n_o m_p)^{0.5}$

where u_m=hotspot internal energy density estimated from equipartition assumptions, n_o=particle (proton) density, m_p=proton mass. In the brighter western hotspot the minimum energy density, assuming equal energy in the protons and electrons is $u_m = 8.5 \times 10^{-8} ergscm^{-3}$; and for ambient particle density, $n_o \sim 10^3 cm^{-3}$ at $10^4 K$ this gives $v = 0.02c$. Such low speeds would not be unexpected for a hotspot formed by a jet whose power has been degraded by strong interaction with obstacles in the ambient medium.

5. Conclusion

We present a very high quality image of 3C179, a bright superluminal quasar with double radio lobes. It has a bright core and a knotty one–sided jet which is initially well–collimated and then appears to be disrupted and split at a splash knot. The jet disruption could be due to interaction of the jet with dense clumpy matter in the IGM. If the nuclear jet and the mas–scale jet have the same inclination angle, θ with respect to the line of sight, then relativistic beaming considerations indicate that the kpc–scale jet is mildly relativistic with $\gamma \sim 1.2 - 1.6$ ($\beta = 0.6 - 0.8$). This can easily be reconciled with lobe distance asymmetry if the speed of the jet has been reduced by $\sim 40\%$ as a result of the splash at knot K_5. It also agrees with an estimated hotspot advance speed $v \sim 0.02c$ for the brighter hotspot. If the hotspot advance speed is decoupled from the jet speed then we need not invoke relativistic considerations to explain the hotspot asymmetry.

Acknowledgements. I have benefitted from very stimulating discussion with Drs A Kus and L. Baath. I am also grateful to Prof R.D. Davies, Director, NRAL for encouragement and access to MERLIN archive data and Prof. R. Booth, Director, OSO for encouragement. The award of the Luverhulme fellowship at Jodrell Bank and the Swedish NFR fellowship at Onsala are gratefully acknowledged.

References

Akujor, C.E. & Garrington, S.T., 1991, *MNRAS*, **250**, 644.
Baars, J.W.M., Genzel, R., Pauliny–Toth, I.I.K. & Witzel, A., 1977. *A&A*, **61**, 99.
Baan, W.D.:1980, *ApJ*, **239**, 433.
Blandford, R & Rees, M.J. 1974, *MNRAS*,**169**, 395.
Chan, K.L. & Henrikson, R.N., 1980, *ApJ*, **241**, 534.
Cornwell, T.J. & Wilkinson, P.N., 1981, *MNRAS*, **196**, 1067.
Hardee, P.E., 1982, *ApJ*, **257**, 509.
Kuhr, H. *et al*, 1981, MPIfR preprint no. 55.
Laing, R.A., 1989, in *Hotspots in Extra–galactic Radio Sources*, eds K. Meisenheiner & H. -P. Roser, Springer–Verlag, Berlin, p.27.
Lind, K.R. & Blandford, R.D., 1985, *ApJ*, **295**, 358.
Lonsdale, C.J.: 1989, in *Hotspots in Extra–galactic Radio Sources*, eds K. Meisenheiner & H. -P. Roser, Springer–Verlag, Berlin, p. 45.
Lonsdale, C.J. & Barthel, P.D., 1984, *A&A*, **135**, 45.
Lonsdale, C.J. & Barthel, P.D., 1986, *AJ.*, **92**, 12.
McCarthy, P.J., 1989*PhD Thesis, University of California.*
Orr, M.J.L. & Browne, I.W.A., 1982, *MNRAS*, **200**, 1067.
Owen, F.N. & Puschell, J.J., 1984, *AJ*, **89**, 932.
Pearson, T.J., Readhead, A.C.S. & Barthel, P.D., 1987, in *Superluminal Radio Sources*, eds J.A. Zensus & T.J. Pearson, Cambridge University Press, p.94.
Perley, R.A., Dreher, J.W. & Cowan, J.J., 1984, *ApJ*, **285**, L35.
Porcas, R.W., 1981, *Nat*, **294**, 47.
Porcas, R.W., 1984, *IAU Symposium 110*, eds R. Fanti *et al.*, D. Reidel, Dordrecht, p.157.
Porcas, R.W., 1986, *IAU Symposium 119*, eds. G. Swarup & V. K. Kapahi, D. Reidel, Dordrecht, p.29.
Porcas, R.W., 1986a, *Mitt. Astron. Ges.*, **65**, 95.
Porcas, R.W., 1987, in *Superluminal Radio Sources*, eds J.A. Zensus & T.J. Pearson, Cambridge University Press, p.12.
Scheuer, P.A.G. & Readhead, A.C.S.:1979, *Nat*, **227**, 182.
Shone, D.L., Porcas, R.W. & Zensus, J.A.: 1985, *Nat*, **314**, 603.
Thomasson, P., 1986. *QJRAS*, **27**, 413.
van Breugel, W., Miley, G., Heckman, T., Butcher, H. & Bridle, H.: 1985, *ApJ*, bf 290, 496.
Wilkinson, P.N., Tzioumis, A.K., Benson, J.M., Walker, R.C., Simon, R.S. & Kahn, F.D., 1991, *Nat*, **352**, 313.
Wills, D. & Wills, B.J. 1976, *ApJS*, **31**, 143.
Zensus, J.A., Porcas, R.W., Pauliny–Toth, I.I.K.:1984, *A&A*, **133**, 27.

This article was processed by the author using Springer-Verlag LaTeX A&A style file 1990.